

# Brain Scaling In Evolved Braitenberg Vehicles

## Abstract

We provide an analysis of how neural dynamics change as a function of brain size in simulated agents. The agents had neural network controllers optimized to solve the Braitenberg phototaxis task. We specifically consider the role of transient dynamics in orientation behavior. We find that the relationship between transience of behavior and brain size is far from intuitive. We found that although reliance on transience We suggest that this toy model may be useful as the reverse engineering approach to cognition continues to grapple with foundational theoretical questions.

## Introduction

The use of artificial neural network models to study cognition goes back to the very origins of the artificial intelligence (cite). However, the average computational capabilities have exploded since that time (cite). The ability to simulate larger and more complex networks has had a major impact on the field of neuroscience. The most recently popularized incarnation of this research program, the Reverse Engineering approach, has emphasized the importance of large scale models in being able to connect theory to experimental data (cite).

One limitation of this approach is the trade-off between tractability and model complexity. As models have more moving parts the harder it becomes to characterize and predict the relationships between those parts.

In much previous work such as in the evolutionary robotics literature (cite), toy models were used to gain theoretical insight. These models were then used to inform the development of experimental models in less complex organisms (cite). Although even in the simplest nervous systems we know of the number of components still seems intractable (cite). Bridging the gap between simpler models with a countable number of components and contemporary models of the Ventral visual stream for example, seems like a daunting and potentially sysiphusian task.

However, sudge a bridge is necessary to build if we are to begin to unravel one of the greatest scientific mysteries that still remains: our own minds. Toy models have given us important insights into which components are important to

driving behavior in cognitive systems, such as the importance of brain, body, environment interactions in shaping cognition (cite). Many of these insights are still on their way to being incorporated into the canon of the reverse engineering approach.

In this study we present an example of how future work may be pursued to connect these varied and important bodies of literature. We consider the effects of scaling in brain size to get a better understanding of how model complexity may affect our understanding of systems of interest. We show that model complexity is not simply a function of the brain size but also deeply depends on the task for which the system is optimized for.

## Reverse Engineering Braitenberg Vehicles

Braitenberg vehicles (cite) are commonly used as a model for

## Related Work

### Methods

The goal of this paper is to study the effect of network size on neural dynamics. To do this we evolved neural network controllers of different sizes to accomplish the same task with the same bodies. This section describes the tasks, the neural network model, the evolutionary optimization algorithm and finally the analysis methodologies used in this work.

### The Task

In all cases the parameters for a neural network were evolved to solve a Braitenberg tropotaxis task. The task consisted of 8 different initial conditions. In each case the agent was initially placed in the center of a circle, with radius  $r = 5$ , which is spanned by evenly spaced stimuli. Each stimulus was present for one trial. An agent's fitness was a function of their proximity to the each stimulus weighted by the time spent during the trial. Agents with maximum fitness were thus those that could arrive at the stimulus quickly and stay

near it as long as possible.

$$f(agent) = 1 - \frac{\sum_{i=1}^8 \sum_{t=1}^T d(agent, stimuli_i) \cdot r}{T} \quad (1)$$

For ease of evaluation the equation above is clipped to be between [0,1]. Each trial lasted for a duration of  $T = 50$  time units. The agents maximum velocity was constrained to a single distance unit per time unit. The agents have two sensors and two motors. The two sensors each receive the inverse distance to the stimulus as input. The sum of the motor outputs determines the velocity of the agent. The difference between the motor outputs determine the agents angular velocity. The velocities were integrated during stimulation with Euler integration using a step size of 0.01

## Neural Network

For the brain of the agent we use continuous-time recurrent neural networks (CTRNNs) with the following state equation (cite):

$$\tau_i \dot{y}_i = -y_i + \sum_{j=i}^N w_{ji} \sigma(y_j + \theta_j) + s_i I_i \quad (2)$$

where  $y$  is the state of each node in the network.  $\tau$  is time constant for each node (in this case all  $\tau$  are set to 1).  $w_{ji}$  is the connection strength from node  $j$  to node  $i$ .  $\theta$  is a bias term unique to each node. The function  $\sigma = 1/(1 + e^{-x})$ .  $I_i$  is the inputs coming to sensory neuron  $i$  weighted by sensory weight  $s_i$ .

The brain networks are fully connected. The weights are all bilaterally symmetric. Sensory input goes to two neurons in the network. Motor output is read out by a linear readout of the entire network. During simulation the network was simulated using Euler integration with a time-step of 0.01. This is done in parallel with environmental simulation. We use networks of sizes 2, 4, 8, 16, and 32.

## Evolutionary Algorithm

The parameters of the neural circuits (all terms above) are evolved using a version of the microbial genetic algorithm (cite). The parameters are encoded as a vector of real numbers between [0,1]. At each step two individuals are selected. Their fitness is compared the winner then transfers a random portion of their genes to the loser. The loser then mutates their genome. The mutation is implemented as a random shift on each gene in the genome drawn from a normal distribution with a mean of 0 and a variance inversely proportional to the number of genes.

The population was initialized with 50 individuals. Evolution was performed over the course of 100 generations. We define one generation as 50 tournaments of 2 randomly selected individuals. Geography is induced where competing agents can only be selected from their 4 nearest neighbors along a 1D ring (cite).

The genome contains all parameters described above as well as the linear readout for the motor output. Before being mapped back to parameters each gene in the genome is multiplied by its corresponding weight range. Biases, sensory and neural weights are constrained to a range of [-16,16]. Motor weights were constrained to [-1,1] however motor output was also normalized in the body during simulation to keep constant maximum speed regardless of brain size.

## Results

### Optimized Agents

In all cases we were able to find agents which were successful at the tropotaxis task. The

### Experiment 2

### Experiment 3

## Conclusion

### Self-Organization in Evolution

The idea that the evolutionary process occurs in spurts, jumps, and bursts rather than gradual, slow and continuous changes has been around for over 75 years (?), but has gained prominence as “punctuated equilibrium” through the work of ??. The general idea is that evolutionary innovations are not bestowed upon an existing species as a whole, gradually, but rather by the emergence of *one* better adapted mutant which, by its superiority, serves as the seed of a new breed that sweeps through an ecological niche and supplants the species previously occupying it. The global dynamics thus has a microscopic origin, as shown experimentally, e.g., in populations of *E. Coli* (?).

Such avalanches can be viewed in two apparently contradictory ways. On the one hand we may consider the wave of extinction touching all species that are connected by their ecological relations, a process akin to percolation and therefore suitably described by the language of second-order critical phenomena (?). Such a scenario relies on the *coevolution* of species (to build their ecological relations) and successfully describes power-law distributions obtained from the fossil record (??). There is, on the other hand, a description in terms of *informational* avalanches that does not require coevolution and leads to the same statistics, as we show here. Rather than contradicting the aforementioned picture (?), we believe it to be complementary.

In the following, we set up a scenario in which *information* is viewed as the agent of self-organization in evolving and adapting populations. Information is, in the strict sense of Shannon theory, a measure of correlation between two ensembles: here a population of genomes and the environment it is adapting to. As described elsewhere (?), this correlation grows as the population stores more and more information about the environment via random measurements, implementing a very effective *natural Maxwell demon*. Any time a stochastic event increases the information stored in the

population, a wave of extinction removes the less adapted genomes and establishes a new era. Yet, information cannot leave the population as a whole, which therefore may be thought of as protected by a *semi-permeable membrane* for information, the hallmark of the Maxwell demon. Let us consider this dynamics in more detail.

The simple living systems we consider here are populations of self-replicating strings of instructions, coded in an alphabet of dimension  $\mathcal{D}$  with variable string length  $\ell$ . The total number of possible strings is exponentially large. Here, we consider the subset of all strings currently in existence in a finite population of size  $N$ , harboring  $N_g$  different types, where  $N_g \ll \mathcal{D}^\ell$ . Each *genotype* (particular sequence of instructions) is characterized by its replication rate  $\epsilon_i$ , which depends on the sequence only, while its survival rate is given by  $\epsilon_i/\langle\epsilon\rangle$ , in a “stirred-reactor” environment that allows a mean-field picture. This average replication rate  $\langle\epsilon\rangle$  characterizes the fitness of the population as a whole, and is given by

$$\langle\epsilon\rangle = \sum_i^{N_g} \frac{n_i}{N} \epsilon_i, \quad (3)$$

where  $n_i$  is the *occupation number*, or frequency, of genotype  $i$  in the population. As  $N_g$  is not fixed in time, the average depends on time also, and is to be taken over all genotypes currently living. The total abundance, or size, of a genotype is then

$$s_i = \int_0^\infty n_i(t) dt = \int_{T_c}^{T_e} n_i(t) dt, \quad (4)$$

where  $T_c$  is the time of creation of this particular genotype, and  $T_e$  the moment of extinction. Before we obtain this distribution in Avida, let us delve further into the statistical description of the extinction events.

At any point in time, the fate of every string in the population is determined by the craftiness of the best adapted member of the population, described by  $\epsilon_{\text{best}}$ . In this simple, finite, world, which does not permit strings to affect other members of the population except by replacing them, not being the best reduces a string to an ephemeral existence. Thus, every string is characterized by a *relative* fitness, or *inferiority*

$$E_i = \epsilon_{\text{best}} - \epsilon_i \quad (5)$$

which plays the role of an *energy* variable for strings of information IAL. Naturally,  $\langle E \rangle = 0$  characterizes the *ground state*, or vacuum, of the population, and strings with  $E_i > 0$  can be viewed as occupying *excited* states, soon to “decay” to the ground state (by being replaced by a string with vanishing inferiority). Through such processes, the dynamics of the system tend to minimize the average inferiority of the population, and the fitness landscape of replication rates

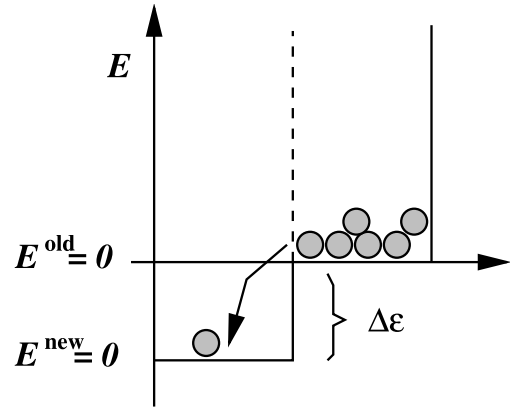


Figure 1: “Energies” (inferiorities) of strings in a first-order phase transition with latent heat  $\Delta\epsilon$ .

thus provides a Lyapunov function. Consequently, we are allowed to proceed with our statistical analysis. Imagine a population in equilibrium, at minimal average inferiority as allowed by the “temperature”: the rate (or more precisely, the probability) of mutation. Imagine further that a mutation event produces a new genotype, fitter than the others, exploiting the environment in novel ways, replicating faster than all the others. It is thus endowed with a new best replication rate,  $\epsilon_{\text{best}}^{\text{new}}$ , larger than the old “best” by an amount  $\Delta\epsilon$ , and redefining what it means to be inferior. Indeed, all inferiorities must now be *renormalized*: what passed as a ground state ( $E = 0$ ) string before now suddenly finds itself in an excited state. The seed of a new generation has been sown, a phase transition must occur. In the picture just described, this is a first-order phase transition with latent heat  $\Delta\epsilon$  (see Fig.1), starting at the “nucleation” point, and leading to an expanding *bubble* of “new phase”.

This bubble expands with a speed given by the Fisher velocity

$$v \sim \sqrt{D\Delta\epsilon}, \quad (6)$$

where  $D$  is the diffusion coefficient (of information) in this medium, until the entire population has been converted (?). This marks the end of the phase transition, as the population returns to equilibrium via mutations acting on the new species, creating new diversity and restoring the *entropy* of the population to its previous value. This prepares the stage for a new avalanche, as only an equilibrated population is vulnerable to even the smallest perturbation. The system has returned to a critical point, driven by mutations, self-organized by information.

Thus we see how a first-order scenario, without coevolution, can lead to self-organized and critical dynamics. It takes place within a single, finite, ecological niche, and thus does not contradict the dynamics taking place for populations that span many niches. Rather, we must conclude that

the descriptions complement each other, from the single-niche level to the ecological web. Let us now take a closer look at the statistics of avalanches in this model, i.e., at the distribution of genotype sizes.

### Exponents and Power Laws

In this particular system avalanche size can be approximated by the size  $s$  of the genotype that gave rise to it, Eq. (4). We shall measure the distribution of these sizes  $P(s)$  in the Artificial Life system Avida, which implements a population of self-replicating computer programs written in a simple machine language-like instruction set of  $\mathcal{D} = 24$  instructions, with programs of varying sequence length. In the course of self-replication, these programs produce mutant off-spring because the `copy` instruction they use is flawed at a rate  $R$  errors per instruction copied, and adapt to an environment in which the performance of *logical* computations on externally provided numbers is akin to the catalysis of chemical reactions (?). In this *artificial chemistry* therefore, successful computations accelerate the metabolism (i.e., the CPU) of those strings that carry the *gene* (code) necessary to perform the trick, and any program discovering a new trick is the seed of another avalanche.

Avida is not a stirred-reactor environment (although one can be simulated). Rather, the programs live on a two-dimensional grid, each program occupying one site. The size of the grid is finite, and chosen in these experiments to be small enough that avalanches are generally over before a new one starts. As is well-known, this is the condition *sine qua non* for the observation of SOC behavior, a separation of time scales which implies that the system is driven at infinitesimal rates.

Let  $\tau$  denote the average duration of an avalanche. Then, a separation of time scales occurs if the average time between the production of new seeds of avalanches is much larger than  $\tau$ . New seeds, in turn, are produced with a frequency  $\langle \epsilon \rangle P$ , where  $\langle \epsilon \rangle$  is again the average replication rate, and  $P$  is the mutation probability (per replication period) for an average sequence of length  $\ell$ ,

$$P = 1 - (1 - R)^\ell. \quad (7)$$

For small enough  $R$  and not too large  $\ell$  (so that the product  $R\ell$  is smaller than unity) we can approximate  $P \approx R\ell$ , and infinitesimal driving occurs in the limit

$$\langle \epsilon \rangle R\ell \ll \frac{1}{\tau}. \quad (8)$$

Furthermore

$$\tau \sim \frac{L}{v} \quad (9)$$

with  $L$  the diameter of the system and  $v$  a typical Fisher velocity. The fastest waves are those for which the latent

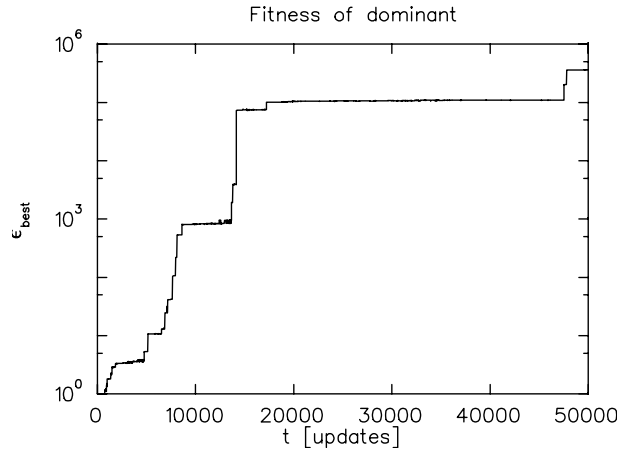


Figure 2: Fitness of the dominant genotype in the population,  $\epsilon_{\text{best}}$  as a function of time (in updates).

heat is of the order of the new fitness, i.e.,  $\Delta\epsilon \sim \epsilon$ , in which case  $v \approx \epsilon$  (because  $D \sim \epsilon$  in Eq. (6), ?), and a separation of time scales is assured whenever

$$\frac{1}{R\ell} \gg L, \quad (10)$$

that is, in the limit of vanishing mutation rate or small population sizes. For the  $L = 60$  system used here, this condition is obeyed (for the fastest waves) only for the smallest mutation rate tested and sequence lengths of the order of the ancestor.

In the following, we keep the population size constant (a  $60 \times 60$  grid) and vary the mutation rate. From the previous arguments, we expect true scale-free dynamics only to appear in the limit of small mutation rates. As in this limit avalanches occur less and less frequently, this is also the limit where data are increasingly difficult to obtain, and other finite size effects can come into play. We shall try to isolate the scale-free regime by fitting the distribution to a power law

$$P(s) \sim s^{-D(R)} \quad (11)$$

and monitor the behavior of  $D$  from low to high mutation rates.

In Fig. 2, we display a typical history of  $\epsilon_{\text{best}}$ , i.e., the fitness of the dominant genotype.<sup>1</sup> Note the “staircase” structure of the curve reflecting the “punctuated” dynamics, where each step reflects a new avalanche and concurrently an extinction event. Staircases very much like these are also observed in adapting populations of *E. Coli* (?).

As touched upon earlier, the Avida world represents an environment replete with information, which we encode by

<sup>1</sup>As the replication rate  $\epsilon$  is exponential in the bonus obtained for a successful computation,  $\epsilon_{\text{best}}$  increases exponentially with time.

providing bonuses for performing logical computations on externally provided (random) numbers. The computations rewarded usually involve two inputs  $A$  and  $B$ , are finite in number and listed in Table 1. At the end of a typical run (such as Fig. 2) the population of programs is usually proficient in almost all tasks for which bonuses are given out, and the genome length has grown to several multiples of the initial size to accommodate the acquired information.

Name	Result	Bonus $b_i$	Difficulty
Echo	I/O	1	—
Not	$\neg A$	2	1
Nand	$\neg(A \wedge B)$	2	1
Not Or	$\neg A \vee B$	3	2
And	$A \wedge B$	3	2
Or	$A \vee B$	4	3
And Not	$A \wedge \neg B$	4	3
Nor	$\neg(A \vee B)$	5	4
Xor	$A \text{ xor } B$	6	4
Equals	$\neg(A \text{ xor } B)$	6	4

Table 1: Logical calculations on random inputs  $A$  and  $B$  rewarded, bonuses, and difficulty (in minimum number of nand instructions required). Bonuses  $b_i$  increase the speed of a CPU by a factor  $\nu_i = 1 + 2^{b_i-3}$ .

Because the amount of information stored in the landscape is finite, adaptation, and the associated avalanches, must stop when the population has exhausted the landscape. However, we shall see that even a ‘flat’ landscape (on which evolution is essentially neutral after the sequence has optimized its replicative strategy) gives rise to a power law of genotype sizes, as long as the programs do not harbor an excessive amount of “junk” instructions. A typical abundance distribution (for the run depicted in Fig. 2) is shown in Fig. 3.

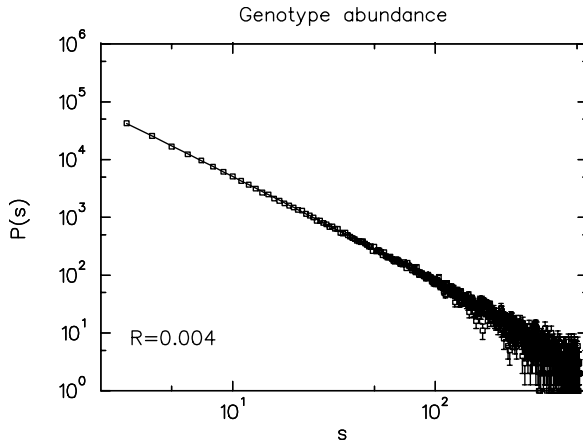


Figure 3: Distribution of genotypes sizes  $P(s)$  fitted to a power law (solid line) at mutation rate  $R = 0.004$ .

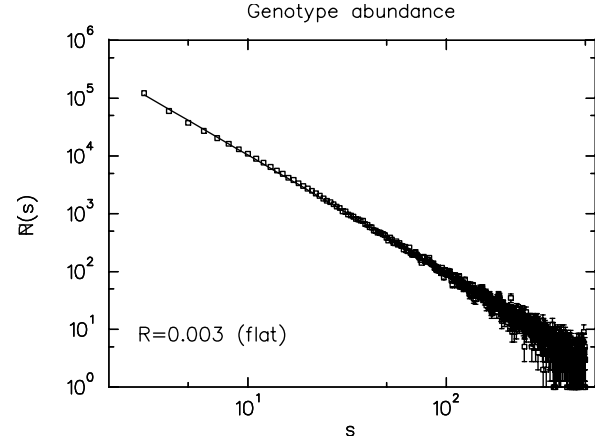


Figure 4: Distribution of genotypes sizes  $P(s)$  for a landscape devoid of the bonuses listed in Tab. 1, at mutation rate  $R = 0.003$ .

As mentioned earlier, we can also turn *off* all bonuses listed in Tab. 1, in which case fitness is related to replicative abilities only. Still, avalanches occur (within the first 50,000 updates monitored) due to minute improvements in fitness, but the length of the genomes typically stays in the range of the ancestor, a program of length 31 instructions. We expect a change of dynamics once the “true” maximum of the local fitness landscape is reached, however, we did not reach this regime in the experiments presented here. The distribution of genotype sizes for the flat landscape is depicted in Fig. 4.

Clearly then, even such landscapes (flat with respect to all other activities except replication) are not neutral. Indeed, it is known that neutral evolution, where the chance for a genotype to increase or decrease in number is even, leads to a power law in the abundance distribution with exponent  $D = 1.5$  (?).

In order to test the dependence of the fitted exponent  $D(R)$  [Eq. (11)] on the mutation rate, we conduct a set of experiments at varying copy-mutation rates from  $0.5 \times 10^{-3}$  to  $10 \times 10^{-3}$  and take data for 50,000 updates. Again, a “best” genotype is not reached after this time, and we must assume that avalanches were still occurring at the end of these runs. Furthermore, in some runs we find that a genotype comes to dominate the population (usually after most ‘genes’ have been discovered) which carries an unusual amount of junk instructions. As mentioned earlier, such species produce a distribution that is exponentially suppressed at large genotype sizes (data not shown). To avoid contamination from such species, we stop recording genotypes after a plateau of fitness was reached, i.e., if the population had discovered most of the bonuses. Furthermore, in order to minimize finite size effects on the determination of the critical exponent, we excluded from this fit all genotype abundances larger than 15, i.e., we only fitted the smallest abundances.

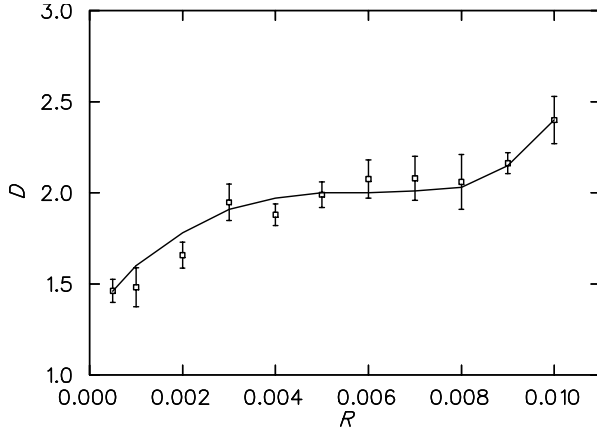


Figure 5: Fitted exponent of power law for 34 runs at mutation rates between  $R = 0.0005$  and  $R = 0.01$  copy errors per instruction copied. The error bars reflect the standard deviation across the sample of runs taken at each mutation rate. The solid line is to guide the eye only.

Indeed, at larger mutation rates the higher abundances are contaminated by a pile-up effect due to the toroidal geometry, while at lower mutation rates a scale appears to enter which prevents scale-free behavior. We have not, as yet, been able to determine the origin of this scale.

In the results reported here, we show the dependence of the fitted exponent  $D$  as a function of the mutation rate  $R$  used in the run, which, however, is a good measure of the mutation probability  $P$  only at small  $R$  and if the sequence length is not excessive. As a consequence, data points at large  $R$ , as well as runs where an excessive sequence length developed, carry a systematic error.

### Acknowledgements

This work was supported by NSF grant No. PHY-9723972.